Development 134, 3259-3269 (2007) doi:10.1242/dev.004267

Novel mutations affecting axon guidance in zebrafish and a role for plexin signalling in the guidance of trigeminal and facial nerve axons

Hideomi Tanaka[1,2,*], Ryu Maeda[1,2,†], Wataru Shoji[2,3], Hironori Wada[1,‡], Ichiro Masai[4,§], Toshiyuki Shiraki[1,5], Megumi Kobayashi[1,2], Ryoko Nakayama[1,5] and Hitoshi Okamoto[1,2,¶]

In zebrafish embryos, the axons of the posterior trigeminal (Vp) and facial (VII) motoneurons project stereotypically to a small number of target muscles derived from the first and second branchial arches (BA1, BA2). Use of the Islet1 (Isl1)-GFP transgenic line enabled precise real-time observations of the growth cone behaviour of the Vp and VII motoneurons within BA1 and BA2. Screening for *N*-ethyl-*N*-nitrosourea-induced mutants identified seven distinct mutations affecting different steps in the axonal pathfinding of these motoneurons. The class 1 mutations caused severe defasciculation and abnormal pathfinding in both Vp and VII motor axons before they reached their target muscles in BA1. The class 2 mutations caused impaired axonal outgrowth of the Vp motoneurons at the BA1-BA2 boundary. The class 3 mutation caused impaired axonal outgrowth of the Vp motoneurons within the target muscles derived from BA1 and BA2. The class 4 mutation caused retraction of the Vp motor axons in BA1 and abnormal invasion of the VII motor axons in BA1 beyond the BA1-BA2 boundary. Time-lapse observations of the class 1 mutant, *vermicelli* (*vmc*), which has a defect in the *plexin A3* (*plxna3*) gene, revealed that Plxna3 acts with its ligand Sema3a1 for fasciculation and correct target selection of the Vp and VII motor axons after separation from the common pathways shared with the sensory axons in BA1 and BA2, and for the proper exit and outgrowth of the axons of the primary motoneurons from the spinal cord.

KEY WORDS: Zebrafish, Trigeminal motoneuron, Facial motoneuron, Plexin A3 mutant, Axon pathfinding

INTRODUCTION

The neuromuscular connection is one of the simplest model systems available for analysis of the mechanisms underlying establishment of functional neural circuits. This system has been used in many studies in vertebrates and invertebrates. Gene knockdown analyses and tissue- and cell-transplantation studies in mouse, chick and zebrafish have revealed that the differentiation and specification of each motoneuron type that innervates target muscles is regulated by the combined temporal expression of transcription factors. These include the LIM-homeodomain-type transcription factors Islet1 (Isl1), Islet2 (Isl2) and Lhx3, and the bHLH-type transcription factors neurogenin 2 and Neuro-M (Appel et al., 1995; Eisen, 1991; Inoue et al., 1994; Landmesser, 2001; Lee and Pfaff, 2003; Segawa et al., 2001; Thaler et al., 2002; Tokumoto et al., 1995; Tsuchida et al., 1994; Uemura et al., 2005). In invertebrates, screening for *Drosophila* mutants showing defects in the axonal pathfinding of motoneurons to specific target muscles has led to the identification of specific ligands and receptors in the neuromuscular connection system, including Semaphorin (Sema)/Plexin (Plex), Slit/Robo, Netrin/Frazzled (a *Drosophila* homologue of mouse Dcc), and receptor protein tyrosine phosphatases (Desai et al., 1996; Johnson and Van Vactor, 2003; Kidd et al., 1999; Kolodkin et al., 1993; Kolodziej et al., 1996; Winberg et al., 1998). Cell adhesion molecules, extracellular matrix molecules, and glycosylated derivatives of these molecules, also participate in the axonal pathfinding process (Birely et al., 2005; Kantor et al., 2004; Keshishian et al., 1996; Schneider and Granato, 2006). The role of these molecules in the regulation of motoneuron axonal pathfinding, the temporal and spatial regulation of these molecules as an integrated system, and the mechanisms underlying their molecular interactions remain unclear.

The jaw muscles of zebrafish embryos are composed of a small number of identifiable muscles derived from the first and second branchial arches (BA1 and BA2) (Fig. 1A,B) (Higashijima et al., 1997; Higashijima et al., 2000; Schilling and Kimmel, 1994; Schilling and Kimmel, 1997). These muscles are innervated by the axons of the anterior and posterior trigeminal motoneurons (Va and Vp) that originate from rhombomeres 2, 3 (r2 and r3), and also by the axons of the facial motoneurons (VII) that originate from r4 (Fig. 1C). The present study shows the stereotypical stepwise outgrowth pattern of the Vp and VII motor axons to target muscles. This was achieved in the Isl1-GFP transgenic strain (Higashijima et al., 2000) using time-lapse observations of axonal pathfinding behaviour of the Vp and VII motoneurons in the lower jaw region of BA1 and BA2, together with laser-mediated cell ablation and

[1]Laboratory for Developmental Gene Regulation, Brain Science Institute, The Institute of Physical and Chemical Research (RIKEN), 2-1 Hirosawa, Wako, Saitama 351-0198, Japan. [2]Core Research for Evolutional Science and Technology (CREST), Japan Science and Technology Corporation (JST), 4-1-8 Honcho, Kawaguchi, Saitama, 332-0012, Japan. [3]Department of Cell Biology, Institute of Development, Aging and Cancer, Tohoku University, Sendai, 980-8575, Japan. [4]Masai Initiative Research Unit, The Institute of Physical and Chemical Research (RIKEN), 2-1 Hirosawa, Wako, Saitama, 351-0198, Japan. [5]Research Resources Center, Brain Science Institute, The Institute of Physical and Chemical Research (RIKEN), 2-1 Hirosawa, Wako, Saitama, 351-0198, Japan.

*Present address: Department of Life Science and Medical Bio-Science, Waseda University, 3-4-1 Okubo Shinjuku-ku, Tokyo, 169-8555, Japan
†Present address: Division of Research and Development, Gene Techno Science Co., Ltd., National Institute of Advanced Industrial Science and Technology (AIST), 2-17, Tsukisamu-Higashi, Toyohira-ku, Sapporo, 062-8517, Japan
‡Present address: Center for Transdisciplinary Research, Department of Environmental Science, Faculty of Science, Niigata University, Ikarashi-2, Nishi-Ku, Niigata 950-2181, Japan
§Present address: Developmental Neurobiology Unit, Initial Research Project, Okinawa Institute of Science and Technology Promotion Corporation, Okinawa Industrial Technology Center, 12-2 Suzaki, Uruma, Okinawa, 904-2234, Japan
¶Author for correspondence (e-mail: hitoshi@brain.riken.jp)

Accepted 12 June 2007

single-cell labelling of the Vp motoneurons. The identification of the genetic loci regulating the stereotypical axonal pathfinding of the Vp and VII motoneurons was achieved by screening mutants. Seven distinct mutant loci leading to specific disruption of the different steps of the axonal pathfinding processes were identified. These mutants were classified into four groups according to the developmental stage in which the axons of the Vp and VII motoneurons began to show abnormal behaviour in the lower jaw region. In addition to abnormal motor axon pathfinding, some mutants displayed other neural defects. In the mutant *vermicelli* (*vmc*), the thick bundle of the Vp and VII motor axons defasciculated into thin branches, with each axon behaving randomly after separation from the common pathway shared with sensory axons. We identified a defect in the gene encoding the zebrafish orthologue of *plxna3* and demonstrated that Plxna3-mediated Sema3a1 signalling is required for the outgrowth of the Vp and VII motoneurons.

MATERIALS AND METHODS

Animals

Zebrafish (*Danio rerio*) were maintained according to standard procedures (Westerfield, 2000). The Isl1-GFP and α-actin-GFP lines, registered as *Tg(CM-isl1:GFP)*^{rw0} and *Tg(α-actin:GFP)*, respectively, in the Zebrafish National BioResource Center of Japan, http://www.shigen.nig.ac.jp/zebra/ (Higashijima et al., 1997; Higashijima et al., 2000), are derived from the RIKEN Wako (RW) wild-type strain. The WIK strain was used for genetic mapping. The embryos were staged according to Kimmel et al. (Kimmel et al., 1995). To prevent pigmentation, embryos were raised in fish water containing 0.0015% *N*-phenylthiourea (PTU; Nakarai) from approximately 12 hours postfertilisation (hpf) (Burrill and Easter, 1994).

Mutagenesis

Mutagenesis was carried out as described previously (Solnica-Krezel et al., 1994; Wada et al., 2005). Mutations were induced in the male germ cells of Isl1-GFP fish using *N*-ethyl-*N*-nitrosourea (ENU; Sigma). To isolate the mutants showing defects in axonal pathfinding of the Vp and VII motoneurons, the embryos from the F2 pairwise crosses were fixed at 72 hpf using trichloroacetic acid (Wako) and stained with anti-acetylated α-tubulin antibody, as described below. The axonal projection patterns of the Vp and VII motoneurons were examined under a dissecting microscope (SMZ1500; Nikon). Of the 1816 haploid genomes (1171 families) screened, three alleles of the *vermicelli* locus (*vmc*^{rw260}, *vmc*^{rw314} and *vmc*^{rw413}), one allele of the *keep off* locus (*kof*^{rw309}), one allele of the *mekong* locus (*mkn*^{rw656}), one allele of the *blue nile* locus (*bln*^{rw646}), three alleles of the *rio grande* locus (*rgd*^{rw218}, *rgd*^{rw395} and *rgd*^{rw520}), one allele of the *loose end* locus (*loe*^{rw357}), and one allele of the *trespassing* locus (*tps*^{rw453}) were identified. To confirm the allelic group, we performed complementation analysis within phenotypically related mutations.

Genetic mapping of the mutation loci

Homozygous embryos (708 of *vmc*, 438 of *kof*, 474 of *mkn*, 1068 of *bnl*, 794 of *rgd*, 480 of *loe* and 460 of *tps*) were selected from the heterozygous parents, which themselves were made by crossing the heterozygous mutant fish with the wild-type WIK strain. Genomic DNA was extracted from individual embryos at 72 hpf, which were fixed and stained with anti-acetylated α-tubulin antibody as described below. To assign the locus of the mutation to a linkage group, we first performed bulk segregant analysis. We then refined the mapping position by scoring meiotic recombination frequency using simple sequence-length polymorphism (SSLP) markers. The positions of SSLP markers were confirmed using the ENSEMBL genome assembly database. The genetic locus of each mutation is shown in Fig. 3. We also confirmed the positions of mutation loci by LN54 radiation hybrid panel using the closest (<0.1 cM) SSLP markers. The linkage group and the positions in the radiation hybrid map are indicated for each mutant in Table 2. By comparison with the known mutation loci registered in Zebrafish Information Network (ZFIN) database, we found that all our mutants were novel.

Table 1. The antisense morpholino oligonucleotides (AMOs) used in this study

plxna3 AMO	5′-TACCAGCAGCCACAAGGACCTCATG-3′
plxna3 AMO-5mis	5′-TACaAGgAGCCAgAAGGAgCTaATG-3′
sema3f1 AMO	5′-ACCCACAAGAGATTTATCAGTCCTA-3′
sema3f1 AMO-5mis	5′-ACgCAgAAGAcATTTATCAcTCgTA-3′
sema3f2 AMO	5′-CATAGACTGTCCAAGAGCATGGTGC-3′
sema3f2 AMO-5mis	5′-CATAcACTcTCgAAGAGgATGcTGC-3′
nrp1b AMO	5′-ACACAGAGCAAACACCAGTACATCC-3′
nrp1b AMO-5mis	5′-ACAgAGAcCAAAgACCAcTAgATCC-3′
nrp2a AMO	5′-CTTGGTGTGATATCCAGAAATCCAT-3′
nrp2a AMO-5mis	5′-CTTcGTcTGATATgCAGAAtTCCgAT-3′
nrp2b AMO	5′-CGCGTAGAGGAAAAAGCTGAAGTTC-3′
nrp2b AMO-5mis	5′-CGCcTAcAGcAAAAAGCTcAAcTTC-3′

Mispaired residues in the control AMOs (AMO-5mis) are indicated in lowercase.

Cloning and sequencing of *plxna3* cDNA

To confirm the nucleotide substitution within the *plxna3* gene, total RNA was extracted from homozygous *vmc* embryos at 72 hpf (*vmc*^{rw260}, *vmc* ^{rw314} and *vmc*^{rw413}) using the RNA Extraction Kit (Nippon Gene), and cDNA was synthesised using the SuperScript III One-Step RT-PCR System with Platinum Taq DNA Polymerase (Invitrogen). The primers used to synthesise full-length *plxna3* cDNA were designed according to genomic sequences from the genome database of the Sanger Centre, Cambridge, UK: sense, 5′-CTGGGACCAACATGGCATTTCC-3′ and antisense, 5′-TCAGCTG-CTGCCAGACATCAG-3′.

Gene knockdown by antisense morpholino oligonucleotides

The antisense morpholino oligonucleotides (AMOs) were designed (by Gene Tools, LLC) to target the first initiation codon of each gene: for AMO sequences, see Table 1. *plxna4*, *sema3a1*, *sema3a2* and *nrp1a* AMOs have been described previously (Miyashita et al., 2004; Sato-Maeda et al., 2006; Yu and Moens, 2005). Approximately 1 nl of AMO (2 mg/ml) was injected into one- to two-cell stage embryos, as described previously (Nasevicius and Ekker, 2000).

In situ hybridisation, immunohistochemistry and rhodamine-phalloidin staining

In situ hybridisation was performed essentially as described previously (Westerfield, 2000) using RNA probes for *isl1*, *isl2*, *plxna3*, *plxna4*, *sema3a1*, *sema3a2*, *sema3f1*, *sema3f2*, *nrp1a*, *nrp1b*, *nrp2a* and *nrp2b*. Immunohistochemistry, using a cocktail of znp-1 antibody and zn-1 monoclonal antibody that recognises primary motoneurons (Oregon Monoclonal Bank; 1:200 and 1:50, respectively), or anti-Kaede polyclonal antibody (MBL; 1:50), was performed according to standard procedures (Westerfield, 2000). For immunohistochemistry using anti-acetylated α-tubulin (Sigma; 1:2000), the embryos were fixed at 72 hpf for 2 hours at room temperature, according to the protocol kindly provided by Dr Stephen W. Wilson (University College London, UK), using 2% trichloroacetic acid in 0.1 M phosphate buffer (pH 7.3), followed by treatment as described above. For the secondary antibody, anti-mouse IgG conjugated to Alexa-488, anti-rabbit IgG conjugated to Alexa-532 (Invitrogen; 1:500) and Histofine Simple Stain MAX-PO (M) (Nichirei) were used. Rhodamine-phalloidin staining was performed according to a previously described procedure (Higashijima et al., 2000). Specimens were visualised by laser-scanning confocal microscopy (LSM 510; Zeiss).

DiI labelling

Anterograde and retrograde labelling of the Vp axons was performed using 2 mg/ml 1,1′-dioctadecyl-3,3,3′,3′-tetramethylindocarbocyanine perchlorate (DiI) dissolved in 100% dimethylformamide. Before labelling, embryos at 70 hpf were anesthetised and embedded in 1.2% low melting point agarose. DiI solution was then applied to the peripheral axons of the Vp motoneurons using a pressure injector (IM300; Narishige). DiI-injected embryos were incubated for 2 hours at 28.5°C, and labelled axons were observed by laser-scanning confocal microscopy.

Single-cell labelling by transient mosaic expression of GFP or Kaede

The CMICP-GFP plasmid (Higashijima et al., 2000) (for consistency with the name of the transgenic line, this is referred to here as the Isl1-GFP plasmid) was used to drive expression of GFP under the control of the enhancer of the *isl1* gene in most cranial motoneurons. The HuC-Kaede plasmid (Sato et al., 2006) was used to drive expression of Kaede in most neurons under the control of the *HuC* (also known as *elavl3* – ZFIN) promoter. The plasmid Isl1-GFP at 10 to 50 ng/μl, or the plasmid HuC-Kaede at 5 ng/μl, was pressure injected into one-cell stage zebrafish embryos. Kaede protein emits green fluorescence that can be converted to red fluorescence by the irradiation of ultraviolet (UV) or violet light (Ando et al., 2002). To observe stochastically Kaede-labelled motoneurons in the Isl1-GFP embryos, Kaede was photoconverted by irradiation of the whole embryo with UV light for 1 to 2 seconds using an upright epifluorescence microscope (Axioplan; Zeiss) with an Achroplan 40× (NA 0.80) water-immersion objective. Selected embryos were fixed and stained with anti-Kaede antibody as described above. To observe GFP-labelled neurons, the embryos were anesthetised and embedded in 1.0% low melting point agarose. The axonal projection patterns of the labelled neurons were then examined using the laser-scanning confocal microscope.

Sequential time-lapse *z*-stack imaging of the multiple mutant embryos

Time-lapse *z*-stack imaging of multiple live mutant embryos was performed using a procedure we developed for sequential time-lapse observation of multiple samples with the laser-scanning confocal microscope equipped with an electric motor-driven stage (MCU28; Zeiss) (for details, see Fig. S3 in the supplementary material). Sequential *z*-stack images (1 μm intervals, 30 focal planes) of six embryos were collected automatically every 15 minutes for 12 to 24 hours using the software supplied with the LSM510 (Multi Time Series Rev. 3.2p). All images were obtained using a Plan-NEOFLUAR 20× (NA 0.50) objective.

Laser-mediated cell ablation

Isl1-GFP transgenic zebrafish embryos were used for laser-mediated cell ablation. Anesthetised 48-hpf embryos were embedded in 1.2% low melting point agarose. The cluster of the Vp motoneurons was then killed using a Micropoint dye laser-mediated cell-ablation system (VSL-337ND; Laser Science) with Coumarin440 nitrogen-pumped dye (peak wavelength 445 nm) attached to an upright epifluorescence microscope (Axioskop; Zeiss) with Achroplan 63× (NA 0.90) water-immersion objective. Irradiation of the Vp cluster with five or six laser pulses was performed until the GFP signals disappeared. After irradiation, we observed the axonal pathfinding behaviour of the intact Vp neurons on the non-operated contralateral side using the laser-scanning confocal microscope. Images were captured every 2 hours from 48 hpf to 62 hpf, and at 72 hpf.

RESULTS

The Vp and VII motoneuron axons project sequentially to target muscles within BA1 and BA2 in a stereotypic stepwise manner

Time-lapse observations of the growth of the Vp and VII motor axons were made using Isl1-GFP transgenic embryos expressing GFP in the cranial motoneurons under the control of the motoneuron-specific enhancer of the *isl1* gene (Higashijima et al., 2000). Time-lapse observations were also made using the double-transgenic embryos for Isl1-GFP and α-actin-GFP, which expressed GFP in both motoneurons and muscles.

By 52 hpf, the Vp motoneuron axons extended ventrally along the pathway in BA1 shared by the sensory trigeminal axons (Fig. 1B, thick black arrow), then separated from the common pathway before extending into the lower jaw region (Fig. 1Da,f,k). At about 54 hpf, the Vp motoneuron axons bifurcated (Fig. 1Db inset, 1Dl) and reached the BA1-BA2 boundary, at which stage the growth cones of the axons extended along the boundary (Fig. 1Db,g, broken line). Concomitantly, the precursors of the intermandibular anterior and the intermandibular posterior muscles started to differentiate around the midline in BA1 (Fig. 1Db,g,l). At 58 hpf, the growth cones of the Vp motoneurons crossed the midline and paused for about 4 hours (Fig. 1Dc,h,m). Then, at approximately 62 hpf, the growth cones on both sides again changed growth direction and extended posteriorly by crossing the BA1-BA2 boundary toward the interhyal muscles derived from BA2 (Fig. 1Dd,i,n). At around 72 hpf, the Vp motor axons completed the projection to the hyohyal muscles in the lower jaw region (Fig. 1De,j,o).

The growth cones of the VII motoneurons also detached from the common pathway shared with the sensory axons in BA2 at about 42 hpf (Fig. 1B, thick white arrow). At approximately 54 hpf, they were near the already differentiated hyohyal muscles derived from BA2 (Fig. 1Db,g,l). From 54 to 58 hpf, the growth cones of the VII motoneurons paused at this position and resumed growth only after 62 hpf (Fig. 1Db-d,g-i,l-n, arrowheads). At about 72 hpf, the VII motoneurons completed the projection to the hyohyal muscles in the lower jaw region (Fig. 1De,j,o).

These observations suggested that both Vp and VII motoneurons projected to their target muscles in a stepwise fashion. Initially, the Vp motoneurons projected to the muscles derived from BA1. During this period, the VII motoneurons did not project to target muscles derived from BA2, even though these muscles were already differentiated. When the initial projection to the BA1-derived muscles was complete, the Vp and VII motoneurons then projected to muscles derived from BA2.

The Vp motoneuron axons bifurcate and project to BA2-derived target muscles on both sides

Time-lapse observations revealed that the growth cones of the Vp motor axons from both sides crossed the midline of the lower jaw region. To examine whether correct axonal pathfinding of the Vp motoneurons from one side depends on interaction with axons from the other side at the ventral midline, the Vp motoneurons on the right side (Fig. 2Aa, arrowhead) were selectively removed at 48 hpf using laser ablation. The outgrowth of the Vp motor axons from the intact side was observed (Fig. 2A). To avoid damage to the Vp neurons on the left side, some of the Vp motoneurons on the right side close to the midline were left intact (Fig. 2Aa-e, brackets). The axons from the laser-irradiated Vp neurons completely degenerated, and the axons from the remaining Vp neurons on the right side did not reach the lower jaw by 72 hpf (Fig. 2Af-j, asterisks). Despite the absence of axons from the contralateral Vp motoneurons, the axons from the intact side showed normal pathfinding behaviour, and projected to the interhyal muscles on both sides in BA2 (Fig. 2Af-j). This result demonstrated that axonal outgrowth of the Vp motoneurons on each side proceeded independently.

We then investigated whether the same or different Vp motoneurons on one side of the hindbrain projected to both the ipsilateral and contralateral lower jaw muscles in BA2. DiI was applied to the common pathway of the Vp axons, and DiI-labelled axons were observed to transfer anterogradely to the interhyal muscles on both sides (Fig. 2Ba, arrowheads). DiI was then applied to the caudal end of the interhyal muscles on one side, which resulted in labelling of the ipsilateral and contralateral branches of the Vp axons innervating the interhyal muscles (Fig. 2Bb, arrowhead). Injection of the Isl1-GFP construct into one-cell stage embryos enabled the transient and stochastic GFP labelling of some of the cranial motoneurons (Fig. 2Ca,b). The GFP-positive axon from a single Vp motoneuron (Fig. 2Ca, arrowhead) was observed

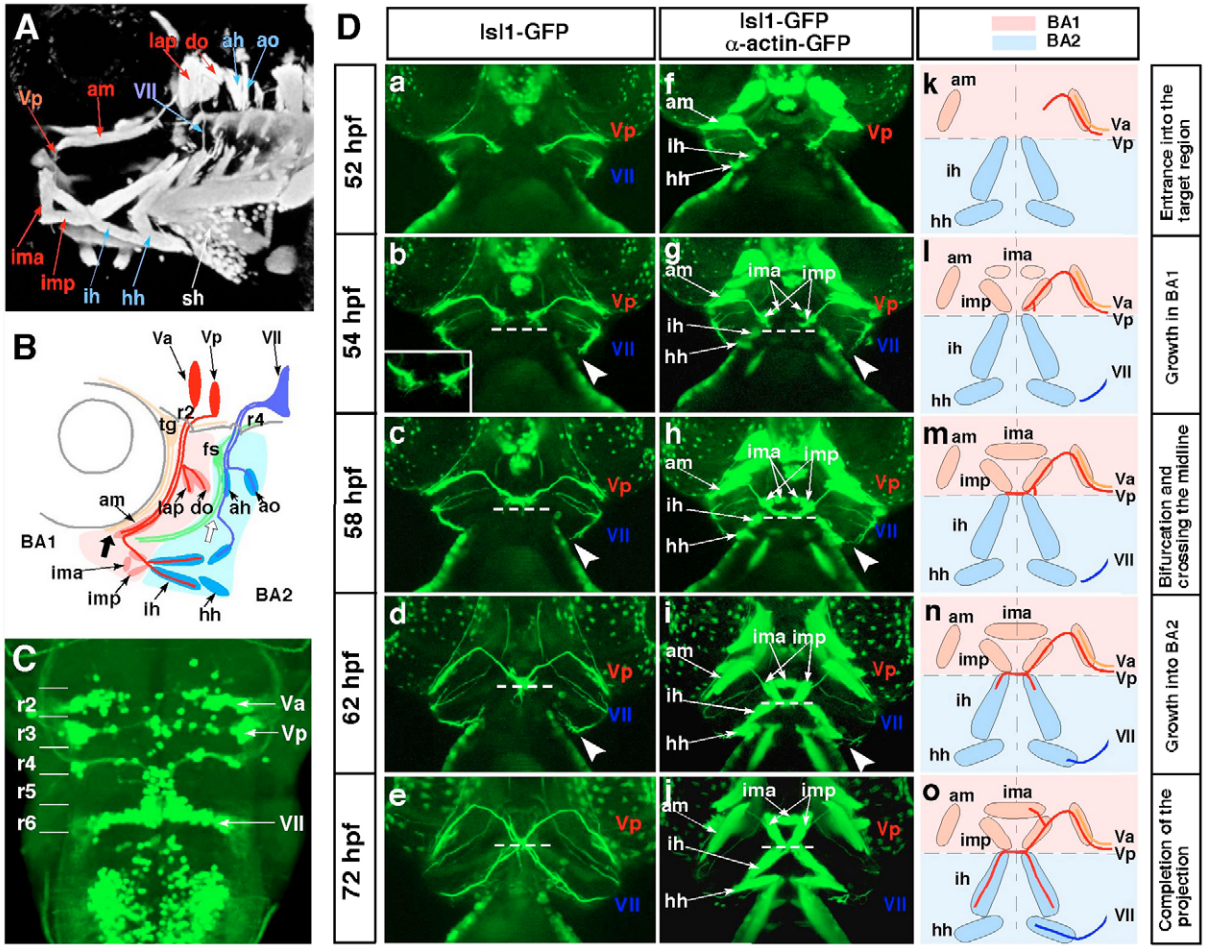

Fig. 1. The stepwise axonal pathfinding of the Vp and VII motoneurons. The cranial axons and jaw muscles were visualised using the Isl1-GFP and α-actin-GFP double-transgenic strain. (**A**,**B**) The jaw region of a 72-hpf zebrafish embryo. Anterior, left. (B) Schematic of the projection pattern of the Va, Vp and VII motoneurons. Thick black and white arrows indicate the points at which these motor axons separate from the common pathways. (**C**) Dorsal view of the hindbrain of a 72-hpf Isl1-GFP transgenic zebrafish embryo. Anterior, top. The Va, Vp and VII motor nuclei are located in r2, r3 and r6, respectively. (**Da-o**) The stepwise outgrowth of the Vp (red) and VII (blue) motoneurons from 52-72 hpf. Ventral view; anterior, top. Broken lines indicate the boundaries between BA1 and BA2 (b-e,g-j). Arrowheads indicate the points at which the growth cones of the VII motoneurons stalled at 54-58 hpf (b-d,g-i). Va, anterior trigeminal motoneurons; Vp, posterior trigeminal motoneurons; VII, facial motoneurons; fs, facial sensory ganglion; tg, trigeminal sensory ganglion; BA1, BA2, first and second branchial arches; r, rhombomere; ah, adductor hyomandibulae; am, adductor mandibulae; ao, adductor operculi; do, dilatator operculi; hh, hyohyal; ih, interhyal; ima, intermandibularis anterior; imp, intermandibularis posterior; lap, levator arcus palatini; sh, sternohyoideus.

to bifurcate and project bilaterally to the interhyal muscles (Fig. 2Cb, arrowheads). These results showed that most of the Vp motoneurons bifurcated at the BA1-BA2 boundary and extended axons to the interhyal muscles on both sides in BA2.

Mutant identification allowed genetic dissection of the stepwise outgrowth of the Vp and VII motor axons into the lower jaw region

To identify the molecules regulating the axonal pathfinding behaviours of Vp and VII motoneurons in BA1 and BA2, we screened ENU-induced mutants with specific defects in these processes. Using complementation analysis, we identified 11 mutations disrupting seven different genes, each affecting the axonal pathfinding behaviour of the Vp and VII motoneurons in a distinctive manner (Fig. 3, Table 2). Each mutation locus was genetically mapped to a distinct location on the chromosome, and these loci did not coincide with any other mutation loci registered in the ZFIN database (Fig. 3). These results were also confirmed using a LN54 radiation hybrid panel (Table 2). Therefore, we concluded that each mutant allele had a novel, distinct mutation locus. These mutations were categorised into four groups according to the developmental stage in which the axons of the Vp and VII motoneurons begin to show abnormal behaviour.

The class 1 mutations included three *vermicelli* (*vmc*^{rw260}, *vmc*^{rw314} and *vmc*^{rw413}) and one *keep off* (*kof*^{rw309}) allele (Fig. 3B,C). The axons of both Vp and VII motoneurons (*vmc* mutants) or of Vp motoneurons alone (*kof* mutant) were defasciculated and extended randomly over target muscles (Fig. 3B,C). The class 2 mutations included one *mekong* (*mkn*^{rw656}), one *blue nile* (*bnl*^{rw646}) and three *rio grande* (*rgd*^{rw218}, *rgd*^{rw395}, and *rgd*^{rw520}) alleles (Fig. 3D-F). In contrast to the class 1 mutants, axons of the Vp motoneurons in the class 2 mutants extended normally through BA1, with the outgrowth of the Vp axons ceasing when the growth extended just past the ventral midline. In these mutants, the axons of the Vp motoneurons did not project to the target muscles in BA2 on either side (Fig. 3D-F). The class 3 mutation included one *loose end* allele (*loe*^{rw357}) (Fig.

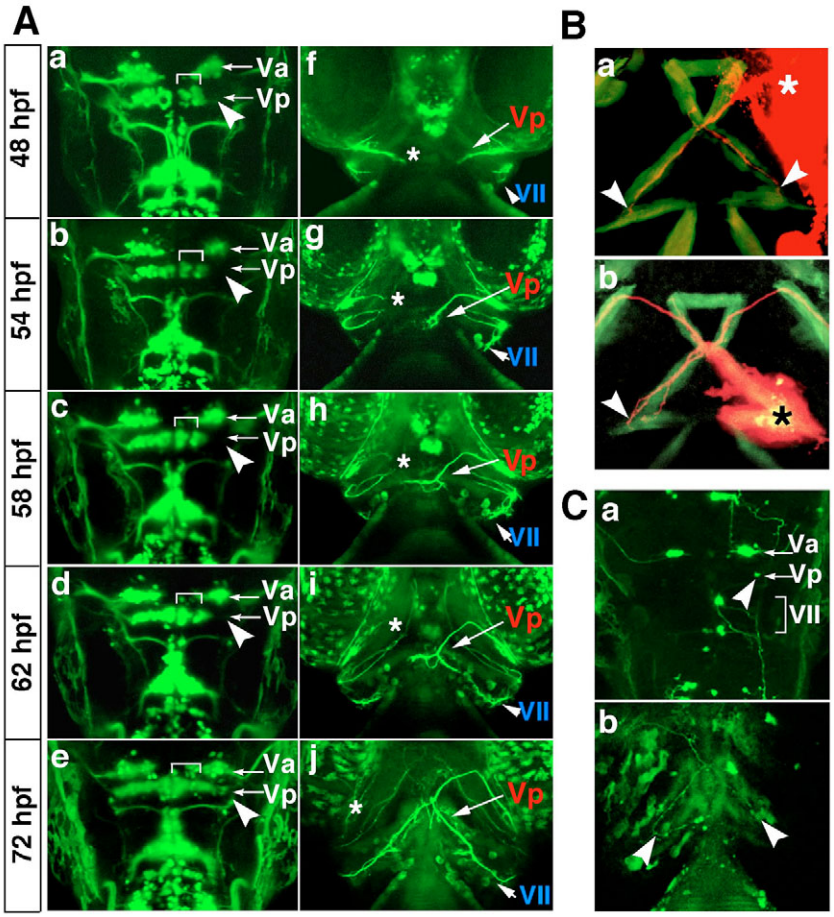

Fig. 2. No interaction is required between the left and right Vp motor axons for projection to the bilateral interhyal muscles in BA2. (**A**) Time-lapse images from 48-72 hpf of the Vp motoneurons after laser irradiation to the lateral part of the Vp motoneurons on the right side (**a-e**, arrowheads). Dorsal (a-e) and ventral (**f-j**) views of the same operated zebrafish embryo. Anterior, top. Brackets indicate remaining cells on the right side (a-e). Asterisks indicate the nerve end of the operated motoneurons (f-j). (**B**) Anterograde (**a**) and retrograde (**b**) labelling of the Vp motor axons of 72-hpf wild-type embryos with DiI. Ventral view; anterior, top. Asterisks indicate the points of DiI application. Arrowheads indicate the ends of the labelled axons. (**C**) Stochastic expression of GFP using the Isl1-GFP construct. Ventral (**a**) and dorsal (**b**) views; anterior, top. Arrowheads indicate a single Vp motoneuron labelled with the Isl1-GFP construct (a) and the ends of the labelled axons (b).

3G). Unlike the class 1 and 2 mutants, the axons of the Vp motoneurons in the *loe* mutant extended along the normal pathway until the BA1-BA2 boundary was crossed, then the growth cones stalled on the way to the caudal end of BA2 (Fig. 3G). The class 4 mutation included one *trespassing* allele (*tps*^{rw453}) (Fig. 3H). In this mutant, the axons of the Vp motoneurons extended initially to the intermandibularis posterior muscles in BA1, then retracted along the path they had grown. The axons of the VII motoneurons extended ectopically as far as the muscles in BA1, by crossing the BA1-BA2 boundary.

In addition to the defects in axonal pathfinding of the Vp motoneurons described above, the *kof*, *bnl* and *rgd* mutations caused defects in the axonal pathfinding of the retinal axons and in differentiation of neurons in the lateral part of the hindbrain and the spinal cord (see Fig. S1 in the supplementary material).

The *vmc* mutation causes severe axonal pathfinding errors of the Vp and VII motoneurons after separation from the common pathways

Time-lapse observations were performed to examine axonal outgrowth of the Vp and VII neurons in the *vmc* embryos (Fig. 4; see Movies S1-6 in the supplementary material). The axons of the VII motoneurons (Fig. 4A, red in the schemes) grew normally along the common pathway within BA2 shared by VII motor axons and facial sensory axons (blue in the schemes) (Fig. 4Aa,e; see Movies S1, S2 in the supplementary material). After separation from the common pathway at 42 hpf, the thick bundle of the VII motor axons defasciculated into thin branches and each axon behaved randomly within BA2 (Fig. 4Ab-d,f-h, arrows; see Movies S1-4 in the supplementary material). The axons of the Vp motoneurons (Fig. 4B, red in the schemes) also grew normally along the common pathway within BA1 that was shared with the trigeminal sensory axons (blue in the schemes). As observed for the VII motoneurons, the Vp motor axons also defasciculated into thin branches and grew randomly over the lower jaw region, whereas the outgrowth of the trigeminal sensory and facial sensory axons remained normal (Fig. 4B; see Movies S5-6 in the supplementary material). These observations suggested that the *vmc* mutation selectively affected the axons of the Vp and VII motoneurons only after they were separated from the common growth pathways and extended towards their target muscles.

The *vmc* locus encodes the zebrafish orthologue of *plxna3*

The mutated *vmc* gene was cloned to elucidate the role of the *vmc* gene product. The *vmc* locus was genetically mapped between the SSLP markers fj56g03 and z15045 on chromosome 8 (Fig. 5A). This locus encodes the zebrafish orthologue of *plxna3*. cDNA fragments of *plxna3* were isolated from total RNA extracted from wild-type and *vmc* homozygous embryos by RT-PCR. A comparison of the cDNA nucleotide sequences of three *vmc* mutants (*vmc*^{rw260}, *vmc*^{rw314} and *vmc*^{rw413}) revealed missense mutations within the regions encoding the Sema domain (*vmc*^{rw260}, E169D), the IPT Plexin repeat 3 domain (*vmc*^{rw314}, C1090S) and the SP domain (*vmc*^{rw413}, W1746R) of Plxna3 (Fig. 5B). In addition, one of the alleles (*vmc*^{rw260}) had an additional nonsense mutation within the Sema-encoding region. There were no significant differences in phenotype between these alleles.

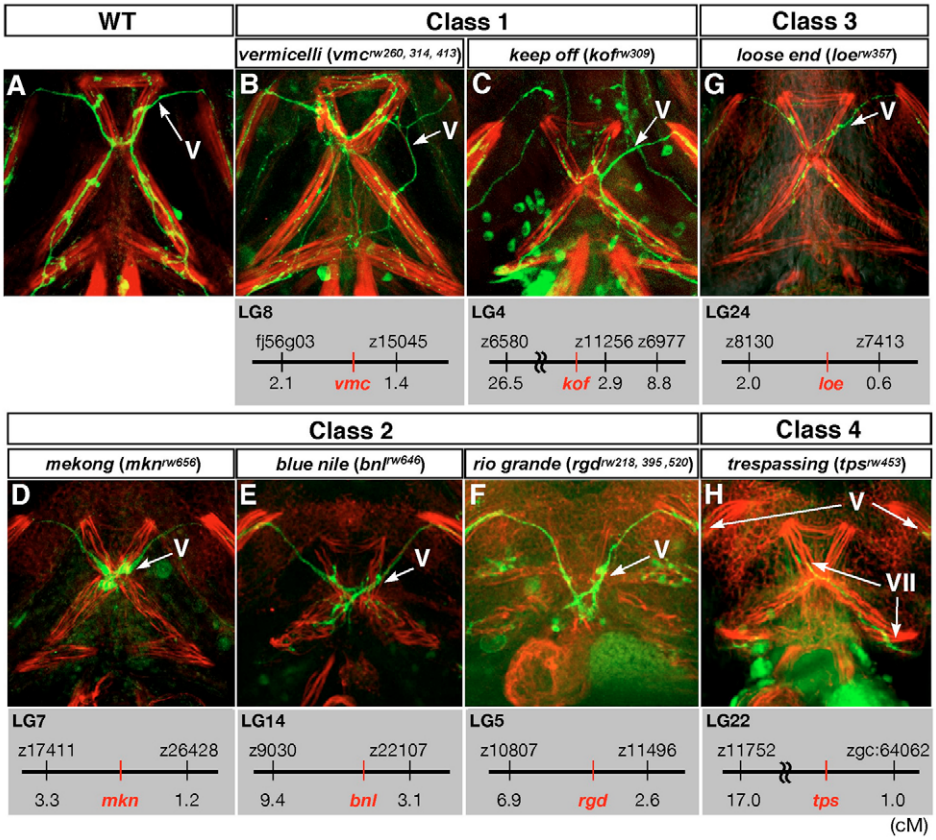

Fig. 3. The projection patterns to the ventral jaw muscles of mutants displaying defects in the outgrowth of the Vp and VII motor axons. Ventral views of the lower jaw of 72-hpf wild-type (**A**) and the four classes of mutant (**B-H**) zebrafish embryos. Anterior, top. The cranial motor axons were labelled with the Isl1-GFP transgene, and each jaw muscle was stained with rhodamine-phalloidin. The genetic locus of each mutation is shown below each panel.

Plxna3 (*vmc*) may act as an essential component of the receptor for Sema3a1 signalling in axonal pathfinding of the Vp and VII motoneurons

A previous study using *plxna3/plxna4* double-knockout mice demonstrated that in sensory and sympathetic neurons, Plxna3 is principally responsible for responses to Sema3f via neuropilin 2 (Nrp2), and Plxna4 is principally responsible for responses to Sema3a via Nrp1 (Yaron et al., 2005). However, there is significant cross association of Plxna3 with Nrp1 and of Plxna4 with Nrp2, which results in involvement of Plxna3 and Plxna4 in mediation of the Sema3a and Sema3f signals, respectively. Therefore, we examined the localisation of the expression of *plxna3*, *plxna4*, *isl1* and *nrp1a* in the cranial motoneurons (Fig. 6Aa-d). Expression of *plxna4* was not observed in the cranial motoneurons, but was possibly present in some interneurons located more dorsolaterally than the cranial motoneurons in the hindbrain (Fig. 6Ad). A previous report demonstrated that *nrp2a* is expressed in the medial part of r2, r3 and r6, which correspond in part to the locations of the Va, Vp and VII motoneurons, and also that *nrp2b* is expressed in a subset of hindbrain neurons in r4 to r6 that may correspond to the VII motoneurons, whereas *nrp1b* is not expressed in the cranial motoneurons (Yu et al., 2004). We found that *plxna3* and *nrp1a* were expressed at 36 hpf in the Va, Vp, and VII motoneurons, similarly to *isl1* (Fig. 6Aa-c). These expression patterns imply that Plxna3 forms a receptor complex with either Nrp1a, Nrp2a or Nrp2b in developing Vp and VII motoneurons. As Nrp1 and Nrp2 preferentially bind to Sema3a and Sema3f, respectively (Takahashi et al., 1999; Yaron et al., 2005), we examined the expression patterns of zebrafish paralogues of *sema3a* and *sema3f* in BA1 and BA2 (Fig. 6B). *sema3a1*, *sema3a2*, *sema3f1* and *sema3f2* (also known as *sema3aa*, *sema3ab*, *sema3fa* and *sema3fb*, respectively – ZFIN) were all expressed in the branchial region (Fig. 6B). *Sema3a2* was expressed in the dorsal part of BA2 and in the boundary region between BA1 and BA2 at 36 and 48 hpf. *Sema3f1* was expressed in the boundary region between BA1 and BA2 at 36 and 48 hpf. S*ema3f2* was weakly expressed in the ventral part of BA2 at 36 and 48 hpf. Among these, the expression of *sema3a1* changed remarkably during development (Fig. 6Ba,e; Fig. 6C). At 36 hpf, expression of *sema3a1* was observed in the posterior margin of BA2 (Fig. 6Ba, arrow; Fig. 6C). By 48 hpf, an additional expression domain appeared in the regions around the adductor mandibulae muscles in BA1 (Fig. 6Be, arrows; Fig. 6C). The temporal expression pattern of *sema3a1* correlates with the timing of the separation of the axons of the Vp motoneurons from the common pathway in BA1 as described above. These findings raise the possibility that Sema3a1 signalling through the Plxna3-Nrp1a, Nrp2a or Nrp2b receptor complexes might be involved in regulation of the axonal growth of the Vp and VII motoneurons in BA1 and BA2.

To test this hypothesis, we examined the knockdown phenotypes using AMOs against all zebrafish paralogues of *plxna3*, *plxna4*, *nrp1*, *nrp2*, *sema3a* and *sema3f* (Fig. 7; see Table S1 in the supplementary material). The embryos injected with these AMOs at the one- or two-cell stage were stained with anti-acetylated α-tubulin antibody at 72 hpf. The embryos injected with the *nrp1a* AMO died early owing to angiogenesis defects, whereas the other morphants developed up to 72 hpf (Fig. 7; see Table S1 in the supplementary material). The *plxna3* and *sema3a1* morphants displayed similar defects in the axonal pathfinding behaviour of both the Vp and VII motoneurons as were observed in the *vmc* embryos (Fig. 7B,D, arrows; Fig. 7E). By contrast, the other morphants showed normal trajectories of the Vp and VII motoneurons (Fig. 7C,E; see Table S1 in the supplementary material). These results suggest that Plxna3 is likely to act as an essential component of the receptor for Sema3a1,

Table 2. Mutations affecting the axonal pathfinding of the Vp and VII motoneurons

Genetic locus	LG (position*)	Alleles	Phenotypes	Other phenotypes
Class 1				
vermicelli (*vmc*)	LG8 (117.9 cR)	*rw260, rw314, rw413*	The axons of both Vp and VII defasciculate and grow randomly on their target muscle regions	
keep off (*kof*)	LG4 (464.0 cR)	*rw309*	The axons of the Vp defasciculate and grow randomly on their target muscle regions	Abnormal formation of the optic chiasm; tail curl down
Class 2				
mekong (*mkn*)	LG7 (22.7 cR)	*rw656*	Axonal growth of the Vp into BA2 is impaired	
blue nile (bnl)	LG14 (297.4 cR)	*rw646*	Axonal growth of the Vp into BA2 is impaired	Isl1-GFP-positive neurons are ectopically induced in the dorsolateral part of r4 to r6 in the hindbrain and in the epibranchial region in BA2. The axons of secondary motoneurons show abnormal trajectory
rio grande (*rgd*)	LG5 (25.5 cR)	*rw218, rw395, rw520*	Axonal growth of the Vp into BA2 is impaired	
Class 3				
loose end (*loe*)	LG24 (156.0 cR)	*rw357*	Axonal growth of the Vp is impaired on their target muscles and projection of the VII to the hyohyal muscles is impaired	
Class 4				
trespassing (*tps*)	LG22 (92.9 cR)	*rw453*	The axons of the Vp retract along the growing pathway in BA1 and the axons of the VII ectopically grow to BA1 crossing the BA1-BA2 boundary	

*Positions of each mutation locus were determined by LN54 radiation hybrid panel using the closest (<0.1 cM) SSLP markers of each mutation locus.

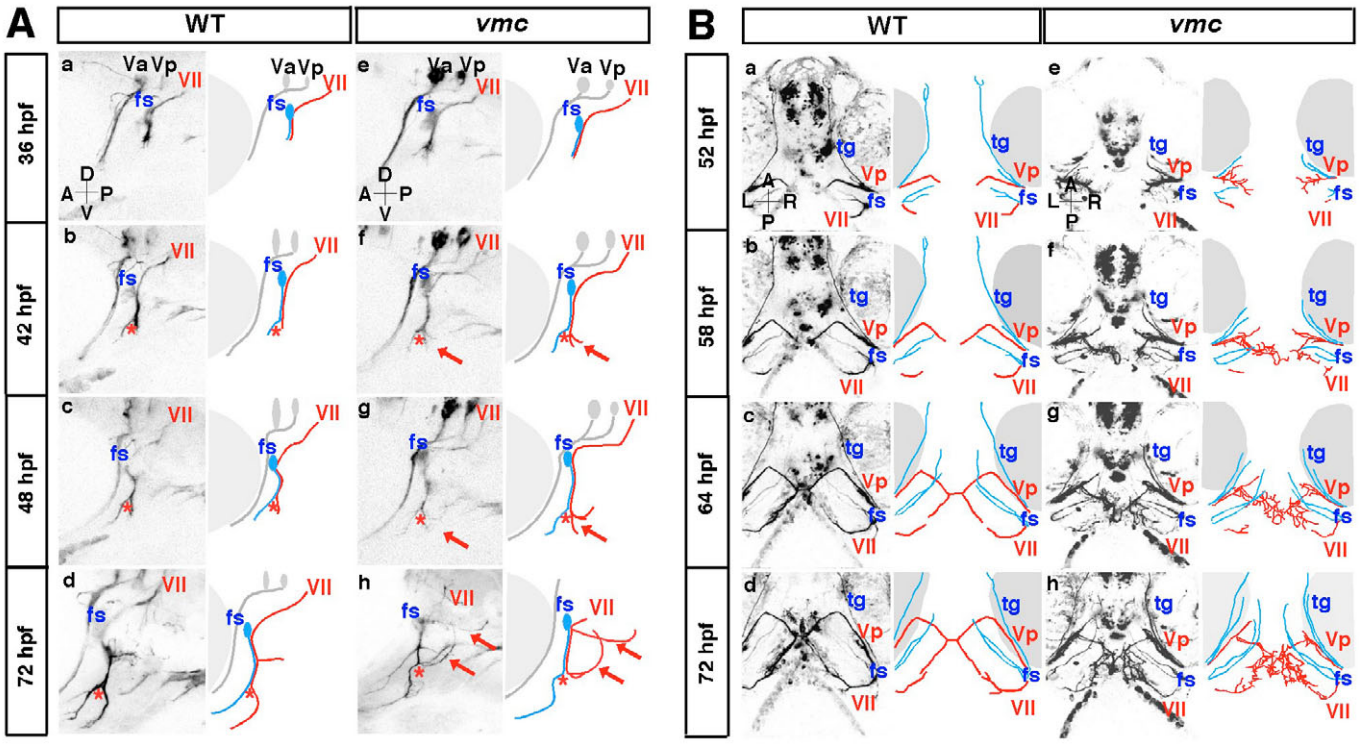

Fig. 4. Time-lapse observations of the axonal outgrowth of the Vp and VII motoneurons in *vmc* embryos. (**A**) Time-lapse images of the axonal outgrowth of the VII motoneurons in wild-type (**a-d**) and *vmc* (**e-h**) zebrafish embryos. Lateral views; anterior, left. The axons of the VII motoneurons (red) and facial sensory (fs) neurons (blue) separated from each other at the points indicated by red asterisks (b-d,f-h). Arrows indicate the abnormal axons (f-h). (**B**) Time-lapse images of the axonal outgrowth of the Vp and VII motoneurons in wild-type (**a-d**) and *vmc* (**e-h**) embryos. Ventral views; anterior, top. The axons of the Vp and VII motoneurons (red) defasciculated into thin axons and grew abnormally (e-h). However, the axons of the trigeminal sensory (tg) and fs neurons (blue) grew normally (e-h).

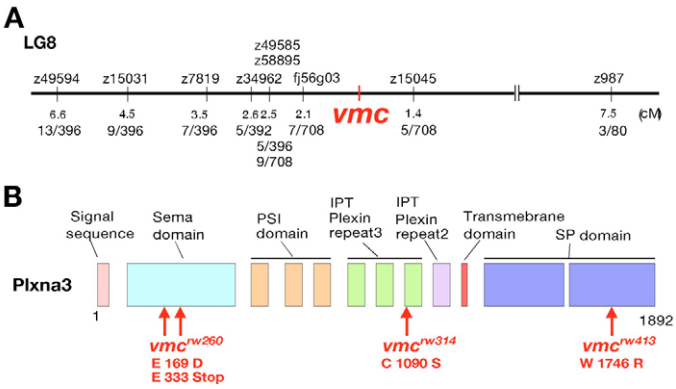

Fig. 5. The genetic locus of *vmc* encodes the zebrafish orthologue of *plxna3*. (**A**) Genetic map of the *vmc* locus. The *vmc* locus was genetically mapped between the SSLP markers fj56g03 (2.1 cM) and z15045 (1.4 cM) on chromosome 8. (**B**) Location of the missense amino acid substitutions in the three *vmc* mutant alleles in the zebrafish orthologue of *plxna3*. Mutations were located within the Sema domain (*vmc*^{rw260}, E169D), in the IPT Plexin repeat 3 domain (*vmc*^{rw314}, C1090S) and in the SP domain (*vmc*^{rw413}, W1746R) of Plxna3. In addition, one allele (*vmc*^{rw260}) carried a stop codon within the Sema domain.

although the involvement of Plxna3 in the Sema3a signal was reported to be rather minor in the axonal pathfinding of the sensory ganglia in mice (Yaron et al., 2005).

Plxna3 (*vmc*) is required for correct axonal pathfinding of primary motoneurons

We found defects in the axonal pathfinding of primary motoneurons in the *vmc* embryos (Fig. 8). The axons of primary motoneurons were visualised by immunohistochemistry, using a cocktail of the znp-1 and zn-1 monoclonal antibodies (Fig. 8A,Be). In the *vmc* embryos, some of the axons extended ventrally out of the spinal cord through the normal exit point (Fig. 8A, arrowheads) then displayed an abnormal trajectory at 28 hpf (Fig. 8Ab, blue arrow). Other axons extended out of the neural tube through ectopic exit points (Fig. 8Ab, red arrows). We also performed single-cell labelling by the transient and stochastic expression of Kaede following injection of the HuC-Kaede plasmid (Sato et al., 2006) into one-cell stage embryos (Fig. 8B). In the wild-type embryos, the axons of primary motoneurons initially grew posteriorly (rostral and middle primary motoneuron, Fig. 8Ba,b) or ventrally (caudal primary motoneuron, Fig. 8Bc) within the spinal cord and extended through the same exit point (Fig. 8B, arrowheads). By contrast, in the *vmc* embryos, some axons grew anteriorly within the spinal cord then extended out of the spinal cord through an abnormal exit point (Fig. 8Bd-f, arrows; see Fig. S2A,B, arrows, in the supplementary material). The expression profile of *plxna3* and *nrp1a* overlapped in all primary motoneuron types (Fig. 8C, asterisks). These findings suggest that Plxna3-dependent signalling is required not only for axonal pathfinding of the Vp and VII motoneurons in the cranial region, but also for pathway selection by the primary motoneurons in the spinal region in zebrafish.

DISCUSSION

In this study, time-lapse observations of the axonal pathfinding of the Vp and VII motoneurons in BA1 and BA2 in the Isl1-GFP transgenic line, revealed that the motoneurons projected to their target muscles in a stepwise fashion. We showed that the axonal pathfinding behaviours of the Vp and VII motoneurons could be genetically dissected into seven distinct mutations. This is the first example of genetic dissection of the axonal pathfinding of the cranial motoneurons in a vertebrate. Among the mutations, we found that the *vermicelli* (*vmc*) locus encodes the zebrafish orthologue of *plxna3*. We also showed that Plxna3 is likely to act as an essential

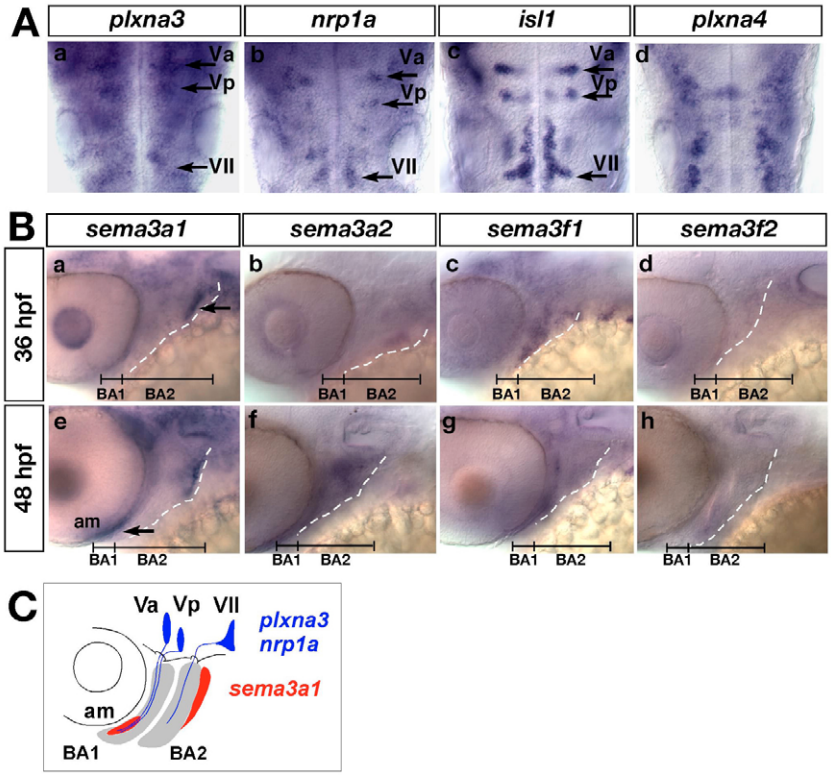

Fig. 6. Expression of the zebrafish orthologues of *plxna3*, *plxna4*, *nrp1a*, *sema3a* and *sema3f* in the cranial region of zebrafish embryos. (**Aa-d**) Expression of *plxna3*, *nrp1a*, *isl1* and *plxna4* mRNA in the cranial motoneurons at 36 hpf. Dorsal views; anterior, top. (**Ba-h**) Expression of *sem3a1*, *sema3a2*, *sema3f1* and *sema3f2* mRNA in the jaw region. Lateral views; anterior, left. Broken lines indicate the posterior margin of BA2. Arrows indicate the expression domains of *sema3a1*. (**C**) Schematic of the expression patterns of *plxna3*, *nrp1a* (blue) and *sema3a1* (red).

component for Sema3a1 signalling for fasciculation and target selection of the extending axons of the Vp and VII motoneurons in zebrafish embryos.

Axonal growth of the Vp and VII motoneurons before separation from the common pathways might be regulated redundantly

The axonal pathfinding of the Vp and VII motoneurons can be divided into two stages. Initially, these motor axons grow along common pathways shared with sensory neuron axons. Subsequently, they separate to extend to their respective target muscles. In the present study, all mutants displayed defects in the later stage of the axonal outgrowth of the Vp and VII motoneurons, after separation from the common pathways. Several redundantly expressed receptor tyrosine phosphatases regulate the separation of the motor axons from the common pathway at the choice point, both in *Drosophila* and in vertebrates (Desai et al., 1996; Johnson and Van Vactor, 2003; Sun et al., 2001; Stepanek et al., 2005; Uetani et al., 2006). Therefore, it is possible that the axonal pathfinding along the common pathway might be regulated by such redundant cues as receptor tyrosine phosphatases.

Class 2 mutant gene products may regulate the boundary crossing of the Vp motoneurons at the BA1-BA2 boundary

The growth cones of the Vp motoneurons paused several hours before they crossed the BA1-BA2 boundary and extended to their target muscles. In the class 2 mutant embryos (*mkn*, *bnl* and *rgd* mutants), growth of the Vp motor axons ceased at the BA1-BA2 boundary and did not resume. The *bnl* and *rgd* mutant embryos also displayed defects in the spinal motoneurons (see Fig. S1 in the supplementary material), suggesting a common mechanism underlying regulation of axonal pathfinding of the Vp motoneurons at the BA1-BA2 boundary and the pathway decision of the spinal motoneurons at the choice point. The zebrafish *unplugged* (*unp*; also known as *musk*) and *diwanka* (*diw*; also known as *plod3*) mutant embryos display cessation of axonal growth of the primary motoneurons at the growth pathway choice point (Schneider and Granato, 2006; Zhang et al., 2004). The *unp* locus encodes muscle-specific kinase, which is implicated in the accumulation of chondroitin sulphate proteoglycans around the choice point (Zhang et al., 2004). The *diw* locus encodes Procollagen-lysine 2-oxoglutarate 5-dioxygenase 3, which glycosylates Col18a1, in the extracellular matrix along the motor path (Schneider and Granato, 2006). Similarly, modification of the extracellular matrix around the choice point may be affected in the *bnl* and *rgd* embryos.

Class 3 and class 4 gene products are required for extension of the Vp motor axons to the target muscles

The class 3 mutant *loe* caused impairment of the axonal outgrowth of the Vp motoneurons on the target muscles in BA1 and BA2. Unlike the other classes of mutants, the growth cones of the Vp motoneurons in the *loe* mutant embryos behaved normally at the BA1-BA2 boundary. Growth was inhibited, but there was no deviation from the normal growth pathway. In the class 4 mutant *tps*, the axons of the Vp motoneurons, which normally grow to the BA1-BA2 boundary, retracted from the boundary region. Concurrently, the axons of the VII motoneurons, which normally never cross the BA1-BA2 boundary, extended to the muscles in BA1 beyond the BA1-BA2 boundary. This observation suggests that the affinity of the growth cones of the Vp and VII motoneurons for the boundary region had changed in the *tps* mutation. Therefore, the molecules encoded by the *loe* and *tps* loci are implicated in the molecular machinery required for the extension of axons to target muscles or in the maintenance of the extended axons, but not in the growth pathway decisions.

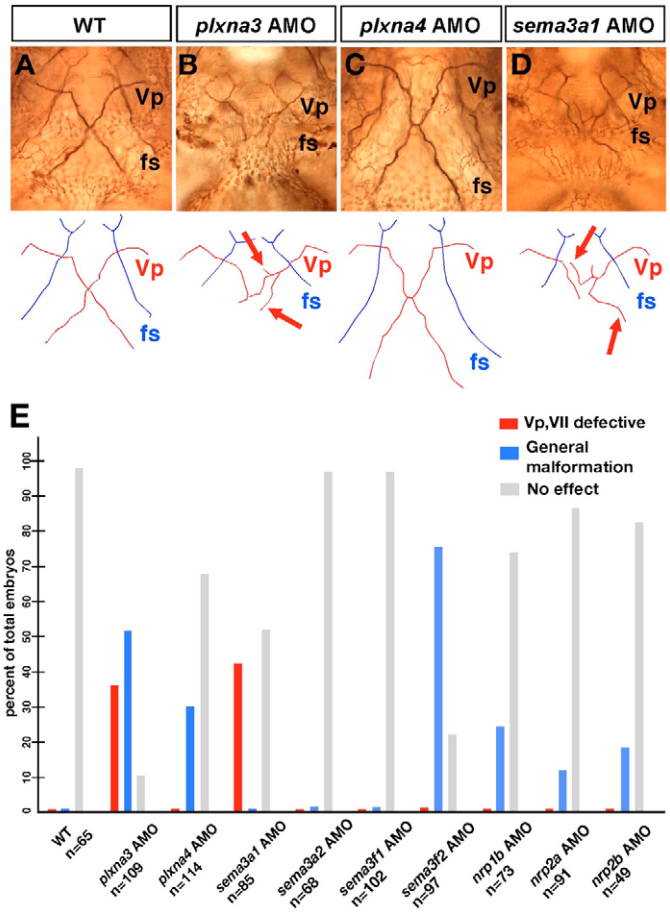

Fig. 7. *Plxna3* (*vmc*) is required for correct axonal pathfinding of the Vp and VII motoneurons. (**A-D**) Projection patterns of the Vp motoneurons in the wild-type embryo and the *plxna3*, *plxna4* and *sema3a1* morphants at 72 hpf. Ventral views; anterior, top. Arrows on schematics below indicate the abnormal trajectories of the defasciculated axons of the Vp motoneurons (B,D). (**E**) Quantitative data for phenotypes of the Vp and VII motoneurons observed in the morphants of the zebrafish orthologues of *plxna3*, *plxna4*, *sema3a*, *sema3f*, *nrp1* and *nrp2*.

Sema3a1/Plxna3 signalling is required for fasciculation and correct axonal pathfinding of the Vp, VII, and the primary motoneurons

In the present study, we identified the *vmc* locus encoded by the zebrafish orthologue of *plxna3*. We also demonstrated that Sema3a1/Plxna3 signalling is necessary for correct axonal pathfinding of the Vp and VII motoneurons. Mice homozygous for a targeted mutation in *Sema3a* or *Nrp1* show severe abnormalities in the peripheral axon projections of cranial and spinal neurons (Kitsukawa et al., 1997; Taniguchi et al., 1997). The loss-of-function phenotype for *Sema3a* signalling causes severe defasciculation and aberrant axonal pathfinding of the lateral motor column motoneurons around the target muscles in mouse and chick (Huber et al., 2005). These phenotypes are similar to the defects in the

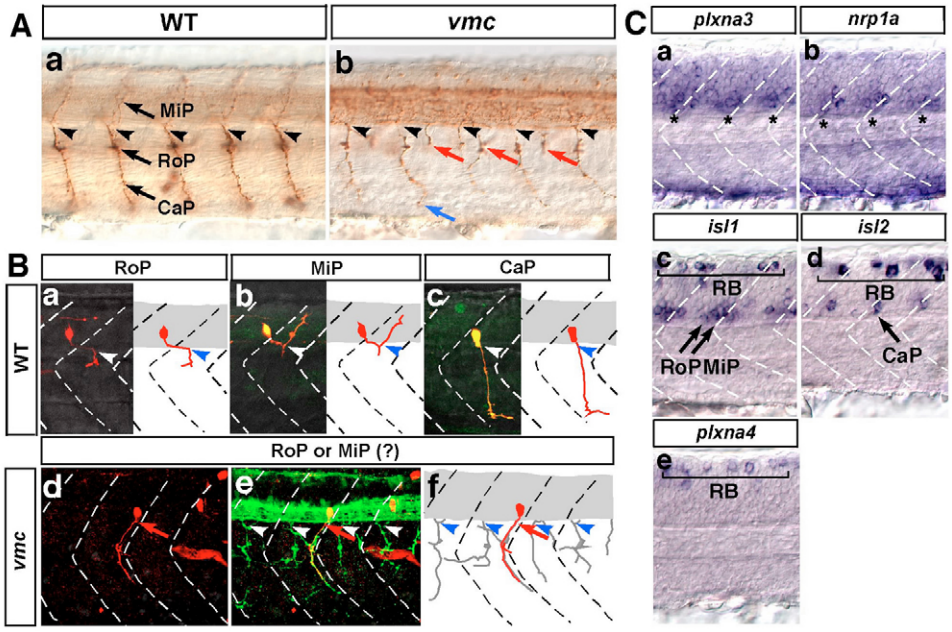

Fig. 8. *Plxna3* (*vmc*) is required for correct axonal pathfinding of the primary motoneurons. (**A**) Axons of primary motoneurons of wild-type (**a**) and *vmc* (**b**) zebrafish embryos at 28 hpf. The blue arrow indicates an axon that showed abnormal pathfinding after extending from the normal exit point. Red arrows indicate axons that extended from the abnormal exit points. (**B**) Kaede-labelled primary motoneurons of wild-type and *vmc* Isl1-GFP embryos at 36 hpf (**a-f**, red). Arrows indicate the axons of RoP- or MiP-like neurons that extended out of the spinal cord through abnormal exit points (d-f). In e, all axons were visualised using a cocktail of znp-1 and zn-1 antibodies (green). Arrowheads in A and B indicate the normal exit points. (**C**) Expression of *plxna3*, *nrp1a*, *isl1*, *isl2* and *plxna4* mRNA in the spinal cord at 24 hpf. Asterisks indicate expression of *plxna3* (**a**) and *nrp1a* (**b**) mRNA. Bracket (**c-e**) indicates Rohon-Beard sensory neurons (RB). In all images, dorsal is top, anterior is left. CaP, caudal primary motoneuron; MiP, middle primary motoneuron; RoP, rostral primary motoneuron.

axonal pathfinding behaviours of the Vp and VII motoneurons in the lower jaw region of the *vmc* embryos. The single-knockout mice for *Plxna3* or *Plxna4* do not show severe defects in the trajectory of efferent fibres in the peripheral nervous system (Cheng et al., 2001; Suto et al., 2005). Severe phenotypes in axonal pathfinding are only observed in *Plxna3*/*Plxna4* double-knockout mice (Yaron et al., 2005). In these studies, the expression of *Plxna3* and *Plxna4* were colocalised in the dorsal root ganglion, the trigeminal ganglion and the sympathetic ganglion (Cheng et al., 2001). By contrast, in zebrafish, the expression domains of *plxna3* and *plxna4* are separate. Plxna3 is expressed mainly in the motoneurons, whereas strong expression of Plxna4 is observed in the sensory neurons (Fig. 8C) (Miyashita et al., 2004). Furthermore, in the present study, axonal pathfinding of sensory neurons was not affected in the *vmc* embryos (Fig. 4). Therefore, we propose that in zebrafish, Plxna3 (but not Plxa4) is likely to act as an essential component of the receptor for Sema3a1 signalling for fasciculation and target selection by the axons of the Vp and VII motoneurons.

In this study, we also found that the axonal pathfinding of primary motoneurons was affected in the *vmc* embryos (Fig. 8). Some axons showed aberrant branching and growth through ectopic exit points. These phenotypes were consistent with the results obtained by other groups (Feldner et al., 2007) (Palaisa and Granato, 2007). In zebrafish embryos, *sema3a1* and *sema3a2* are expressed in each somite (Sato-Maeda et al., 2006; Roos et al., 1999), and genetic interactions of Plxna3 with Sema3a1 and Sema3a2 have been reported (Feldner et al., 2007). Together, these findings suggest that Plxna3 might act as an essential component of the receptor for Sema3a signalling in the axonal pathfinding of the primary motoneurons.

We wish to thank the members of the mutant-screening team in the Okamoto laboratory for their expert technical assistance and fish care, and M. Granato and K. A. Palaisa for communication of unpublished data. This research was supported in part by a Grant-in-Aid from the Ministry of Education, Science, Technology, Sports and Culture of Japan, and grants for Core Research for Evolutional Science and Technology from the Japan Science and Technology Corporation.

Supplementary material

Supplementary material for this article is available at
http://dev.biologists.org/cgi/content/full/134/18/3259/DC1

References

Ando, R., Hama, H., Yamamoto-Hino, M., Mizuno, H. and Miyawaki, A. (2002). An optical marker based on the UV-induced green-to-red photoconversion of a fluorescent protein. *Proc. Natl. Acad. Sci. USA* **99**, 12651-12656.

Appel, B., Korzh, V., Glasgow, E., Thor, S., Edlund, T., Dawid, I. B. and Eisen, J. S. (1995). Motoneuron fate specification revealed by patterned LIM homeobox gene expression in embryonic zebrafish. *Development* **121**, 4117-4125.

Birely, J., Schneider, V. A., Santana, E., Dosch, R., Wagner, D. S., Mullins, M. C. and Granato, M. (2005). Genetic screens for genes controlling motor nerve-muscle development and interactions. *Dev. Biol.* **280**, 162-176.

Burrill, J. D. and Easter, S. S., Jr (1994). Development of the retinofugal projections in the embryonic and larval zebrafish (*Brachydanio rerio*). *J. Comp. Neurol.* **346**, 583-600.

Cheng, H. J., Bagri, A., Yaron, A., Stein, E., Pleasure, S. J. and Tessier-Lavigne, M. (2001). Plexin-A3 mediates semaphorin signaling and regulates the development of hippocampal axonal projections. *Neuron* **32**, 249-263.

Desai, C. J., Gindhart, J. G., Jr, Goldstein, L. S. and Zinn, K. (1996). Receptor tyrosine phosphatases are required for motor axon guidance in the Drosophila embryo. *Cell* **84**, 599-609.

Eisen, J. S. (1991). Determination of primary motoneuron identity in developing zebrafish embryos. *Science* **252**, 569-572.

Feldner, J., Reimer, M. M., Schweitzer, J., Wendik, B., Meyer, D., Becker, T. and Becker, C. G. (2007). PlexinA3 restricts spinal exit points and branching of trunk motor nerves in embryonic zebrafish. *J. Neurosci.* **27**, 4978-4983.

Higashijima, S., Okamoto, H., Ueno, N., Hotta, Y. and Eguchi, G. (1997). High-frequency generation of transgenic zebrafish which reliably express GFP in whole muscles or the whole body by using promoters of zebrafish origin. *Dev. Biol.* **192**, 289-299.
Higashijima, S., Hotta, Y. and Okamoto, H. (2000). Visualization of cranial motor neurons in live transgenic zebrafish expressing green fluorescent protein under the control of the islet-1 promoter/enhancer. *J. Neurosci.* **20**, 206-218.
Huber, A. B., Kania, A., Tran, T. S., Gu, C., De Marco Garcia, N., Lieberam, I., Johnson, D., Jessell, T. M., Ginty, D. D. and Kolodkin, A. L. (2005). Distinct roles for secreted semaphorin signaling in spinal motor axon guidance. *Neuron* **48**, 949-964.
Inoue, A., Takahashi, M., Hatta, K., Hotta, Y. and Okamoto, H. (1994). Developmental regulation of islet-1 mRNA expression during neuronal differentiation in embryonic zebrafish. *Dev. Dyn.* **199**, 1-11.
Johnson, K. G. and Van Vactor, D. (2003). Receptor protein tyrosine phosphatases in nervous system development. *Physiol. Rev.* **83**, 1-24.
Kantor, D. B., Chivatakarn, O., Peer, K. L., Oster, S. F., Inatani, M., Hansen, M. J., Flanagan, J. G., Yamaguchi, Y., Sretavan, D. W., Giger, R. J. and Kolodkin, A. L. (2004). Semaphorin 5A is a bifunctional axon guidance cue regulated by heparan and chondroitin sulfate proteoglycans. *Neuron* **44**, 961-975.
Keshishian, H., Broadie, K., Chiba, A. and Bate, M. (1996). The drosophila neuromuscular junction: a model system for studying synaptic development and function. *Annu. Rev. Neurosci.* **19**, 545-575.
Kidd, T., Bland, K. S. and Goodman, C. S. (1999). Slit is the midline repellent for the robo receptor in Drosophila. *Cell* **96**, 785-794.
Kimmel, C. B., Ballard, W. W., Kimmel, S. R., Ullmann, B. and Schilling, T. F. (1995). Stages of embryonic development of the zebrafish. *Dev. Dyn.* **203**, 253-310.
Kitsukawa, T., Shimizu, M., Sanbo, M., Hirata, T., Taniguchi, M., Bekku, Y., Yagi, T. and Fujisawa, H. (1997). Neuropilin-Semaphorin III/D-mediated chemorepulsive signals play a crucial role in peripheral nerve projection in mice. *Neuron* **19**, 995-1005.
Kolodkin, A. L., Matthes, D. J. and Goodman, C. S. (1993). The semaphorin genes encode a family of transmembrane and secreted growth cone guidance molecules. *Cell* **75**, 1389-1399.
Kolodziej, P. A., Timpe, L. C., Mitchell, K. J., Fried, S. R., Goodman, C. S., Jan, L. Y. and Jan, Y. N. (1996). frazzled encodes a Drosophila member of the DCC immunoglobulin subfamily and is required for CNS and motor axon guidance. *Cell* **87**, 197-204.
Landmesser, L. T. (2001). The acquisition of motoneuron subtype identity and motor circuit formation. *Int. J. Dev. Neurosci.* **19**, 175-182.
Lee, S. K. and Pfaff, S. L. (2003). Synchronization of neurogenesis and motor neuron specification by direct coupling of bHLH and homeodomain transcription factors. *Neuron* **38**, 731-745.
Miyashita, T., Yeo, S. Y., Hirate, Y., Segawa, H., Wada, H., Little, M. H., Yamada, T., Takahashi, N. and Okamoto, H. (2004). PlexinA4 is necessary as a downstream target of Islet2 to mediate Slit signaling for promotion of sensory axon branching. *Development* **131**, 3705-3715.
Nasevicius, A. and Ekker, S. C. (2000). Effective targeted gene 'knockdown' in zebrafish. *Nat. Genet.* **26**, 216-220.
Palaisa, K. A. and Granato, M. (2007). Analysis of zebrafish *sidetracked* mutants reveals a novel role for Plexin A3 in intraspinal motor axon guidance. *Development* **134**, 3251-3257.
Roos, M., Schachner, M. and Bernhardt, R. R. (1999). Zebrafish semaphorin Z1b inhibits growing motor axons in vivo. *Mech. Dev.* **87**, 103-117.
Sato, T., Takahoko, M. and Okamoto, H. (2006). HuC:Kaede, a useful tool to label neural morphologies in networks in vivo. *Genesis* **44**, 136-142.
Sato-Maeda, M., Tawarayama, H., Obinata, M., Kuwada, J. Y. and Shoji, W. (2006). Sema3a1 guides spinal motor axons in a cell- and stage-specific manner in zebrafish. *Development* **133**, 937-947.
Schilling, T. F. and Kimmel, C. B. (1994). Segment and cell type lineage restrictions during pharyngeal arch development in the zebrafish embryo. *Development* **120**, 483-494.
Schilling, T. F. and Kimmel, C. B. (1997). Musculoskeletal patterning in the pharyngeal segments of the zebrafish embryo. *Development* **124**, 2945-2960.
Schneider, V. A. and Granato, M. (2006). The myotomal diwanka (lh3) glycosyltransferase and type XVIII collagen are critical for motor growth cone migration. *Neuron* **50**, 683-695.
Segawa, H., Miyashita, T., Hirate, Y., Higashijima, S., Chino, N., Uyemura, K., Kikuchi, Y. and Okamoto, H. (2001). Functional repression of Islet-2 by disruption of complex with Ldb impairs peripheral axonal outgrowth in embryonic zebrafish. *Neuron* **30**, 423-436.
Solnica-Krezel, L., Schier, A. F. and Driever, W. (1994). Efficient recovery of ENU-induced mutations from the zebrafish germline. *Genetics* **136**, 1401-1420.
Stepanek, L., Stoker, A. W., Stoeckli, E. and Bixby, J. L. (2005). Receptor tyrosine phosphatases guide vertebrate motor axons during development. *J. Neurosci.* **25**, 3813-3823.
Sun, Q., Schindelholz, B., Knirr, M., Schmid, A. and Zinn, K. (2001). Complex genetic interactions among four receptor tyrosine phosphatases regulate axon guidance in Drosophila. *Mol. Cell. Neurosci.* **17**, 274-291.
Suto, F., Ito, K., Uemura, M., Shimizu, M., Shinkawa, Y., Sanbo, M., Shinoda, T., Tsuboi, M., Takashima, S., Yagi, T. et al. (2005). Plexin-A4 mediates axon-repulsive activities of both secreted and transmembrane semaphorins and plays roles in nerve fiber guidance. *J. Neurosci.* **25**, 3628-3637.
Takahashi, T., Fournier, A., Nakamura, F., Wang, L. H., Murakami, Y., Kalb, R. G., Fujisawa, H. and Strittmatter, S. M. (1999). Plexin-neuropilin-1 complexes form functional semaphorin-3A receptors. *Cell* **99**, 59-69.
Taniguchi, M., Yuasa, S., Fujisawa, H., Naruse, I., Saga, S., Mishina, M. and Yagi, T. (1997). Disruption of *semaphorin III/D* gene causes severe abnormality in peripheral nerve projection. *Neuron* **19**, 519-530.
Thaler, J. P., Lee, S. K., Jurata, L. W., Gill, G. N. and Pfaff, S. L. (2002). LIM factor Lhx3 contributes to the specification of motor neuron and interneuron identity through cell-type-specific protein-protein interactions. *Cell* **110**, 237-249.
Tokumoto, M., Gong, Z., Tsubokawa, T., Hew, C. L., Uyemura, K., Hotta, Y. and Okamoto, H. (1995). Molecular heterogeneity among primary motoneurons and within myotomes revealed by the differential mRNA expression of novel islet-1 homologs in embryonic zebrafish. *Dev. Biol.* **171**, 578-589.
Tsuchida, T., Ensini, M., Morton, S. B., Baldassare, M., Edlund, T., Jessell, T. M. and Pfaff, S. L. (1994). Topographic organization of embryonic motor neurons defined by expression of LIM homeobox genes. *Cell* **79**, 957-970.
Uemura, O., Okada, Y., Ando, H., Guedj, M., Higashijima, S., Shimazaki, T., Chino, N., Okano, H. and Okamoto, H. (2005). Comparative functional genomics revealed conservation and diversification of three enhancers of the isl1 gene for motor and sensory neuron-specific expression. *Dev. Biol.* **278**, 587-606.
Uetani, N., Chagnon, M. J., Kennedy, T. E., Iwakura, Y. and Tremblay, M. L. (2006). Mammalian motoneuron axon targeting requires receptor protein tyrosine phosphatases sigma and delta. *J. Neurosci.* **26**, 5872-5880.
Wada, H., Iwasaki, M., Sato, T., Masai, I., Nishiwaki, Y., Tanaka, H., Sato, A., Nojima, Y. and Okamoto, H. (2005). Dual roles of zygotic and maternal Scribble1 in neural migration and convergent extension movements in zebrafish embryos. *Development* **132**, 2273-2285.
Westerfield, M. (2000). *The Zebrafish Book* (4th edn). Eugene, OR: University of Oregon.
Winberg, M. L., Noordermeer, J. N., Tamagnone, L., Comoglio, P. M., Spriggs, M. K., Tessier-Lavigne, M. and Goodman, C. S. (1998). Plexin A is a neuronal semaphorin receptor that controls axon guidance. *Cell* **95**, 903-916.
Yaron, A., Huang, P. H., Cheng, H. J. and Tessier-Lavigne, M. (2005). Differential requirement for Plexin-A3 and -A4 in mediating responses of sensory and sympathetic neurons to distinct class 3 Semaphorins. *Neuron* **45**, 513-523.
Yu, H. H. and Moens, C. B. (2005). Semaphorin signaling guides cranial neural crest cell migration in zebrafish. *Dev. Biol.* **280**, 373-385.
Yu, H. H., Houart, C. and Moens, C. B. (2004). Cloning and embryonic expression of zebrafish neuropilin genes. *Gene Expr. Patterns* **4**, 371-378.
Zhang, J., Lefebvre, J. L., Zhao, S. and Granato, M. (2004). Zebrafish unplugged reveals a role for muscle-specific kinase homologs in axonal pathway choice. *Nat. Neurosci.* **7**, 1303-1309.

Table S1. The phenotypes of morpholino-injected embryos in the axonal pathfinding of the Vp and VII motoneurons

AMO	Total	Vp, VII defective	General malformation	No effect
Wild type	65	0 (0%)	0 (0%)	65 (100%)
plxna3	109	41 (38%)	57 (52%)	11 (10%)
plxna4	114	0 (0%)	35 (31%)	79 (69%)
sema3a1	85	37 (44%)	0 (0%)	48 (56%)
sema3a2	68	0 (0%)	1 (1%)	67 (99%)
sema3f1	102	0 (0%)	3 (1%)	99 (99%)
sema3f2	97	1 (1%)	76 (78%)	21 (22%)
nrp1a	–	–	–	–
nrp1b	73	0 (0%)	18 (25%)	55 (75%)
nrp2a	91	0 (0%)	12 (13%)	79 (87%)
nrp2b	49	0 (0%)	9 (18%)	40 (82%)